Impact Resistance and Secondary Transitions*

BRUCE HARTMANN and G. F. LEE, *Polymer Physics Group, Naval Surface Weapons Center, White Oak, Silver Spring, Maryland 20910*

Synopsis

Instrumented Charpy impact measurements were made on polycarbonate from liquid nitrogen temperature to room temperature. The polymer had a transition from brittle fracture to ductile failure at −130°C. Scanning electron micrographs of the fracture surfaces did not correlate with the secondary transition or test temperature. A Fourier analysis of the impact pulse covers a wide range of frequencies, but the dominant frequencies at room temperature are below 200 Hz. Time–temperature superposition shows that the secondary transition occurs over a broad frequency range centered at 7 MHz at room temperature. Impact strength and the secondary transition (at impact frequency) both have a maximum value around −75°C.

INTRODUCTION

It has been empirically observed[1–3] that high impact resistance at room temperature can be correlated with secondary transitions in glassy polymers. The question immediately arises: Why should a secondary transition, occurring well below room temperature, be related to impact at room temperature? An obvious answer is that an impact stress pulse corresponds to a high-frequency measurement which, by the time–temperature superposition principle, has the effect of raising the secondary transition to higher temperature. Since the dynamic mechanical loss factor is higher in the vicinity of the secondary transition than it is anywhere else except the glass transition, some of the impact energy can be absorbed harmlessly in the form of heat, thus offering protection from fracture.

Boyer[3] has already used time–temperature superposition to calculate the (single) frequency at room temperature of the secondary transition peak. He found a very rough correlation between high impact resistance and high frequency. Sacher,[2] in addition, used the rise time of the impact stress pulse to estimate the (single) frequency corresponding to impact. He found a correlation between high impact resistance and high loss factor. In this paper, we have extended the above approaches by doing a Fourier analysis to obtain the complete frequency spectrum of the impact pulse and comparing this spectrum with the room-temperature frequency spectrum of the loss factor of the secondary transition (calculated with an Arrhenius time–temperature conversion).

Impact measurements were made on polycarbonate as a function of temperature using the Charpy mode (three-point bending) on unnotched specimens so that the results would be indicative of the inherent physical properties of the polymer rather than specimen geometry. The measurements were done on an instrumented impact tester that yields impact stress histories in addition to total fracture energy. Dynamic mechanical loss measurements were made in a tor-

* Presented in part at the VIIth International Congress on Rheology, Gothenburg, Sweden, 1976.

Journal of Applied Polymer Science, Vol. 23, 3639–3650 (1979)

0021-8995/79/0023-3639$01.00

sional pendulum. In addition, fracture surfaces were examined in a scanning electron microscope (SEM) to try to correlate fracture topography with the secondary transition and the temperature dependence of impact.

EXPERIMENTAL

The specimens used in this work were machined from a sheet of commercial polycarbonate (Rohm and Haas Company) of the bisphenol A type, poly(4,4′-dioxydiphenyl-2,2-propane) carbonate, having the structure

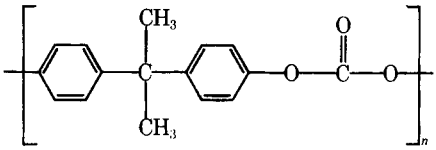

According to the manufacturer, the weight-average molecular weight of this polymer is 27,000, and its number-average molecular weight is 16,000. The measured density of the polymer was 1.20 g/cm^3.

Impact measurements were made at four temperatures: −196, −160, −130, and 25°C. Five specimens were used at each temperature. As-received specimens were conditioned before testing for approximately 45 min in constant-temperature baths. At −196°C, liquid nitrogen was used as the bath medium. At −160°C, liquid nitrogen was used to cool isopentane to a solid–liquid equilibrium mixture. At −130°C, a pentane solid–liquid equilibrium mixture was used. After conditioning, the specimen was removed from the bath, placed in the impact machine (at room temperature), and tested as quickly as possible, about 5 sec.

Impact testing was performed using a Riehle testing machine in the Charpy mode, i.e., allowing a free-swinging pendulum hammer to strike the specimen in a dynamic three-point bending test. A low-capacity pendulum hammer was used at an energy setting of 40.7 J. At this setting, the hammer velocity upon impact with the specimen was 3.4 m/sec. The specimen was 5.5 cm long, 1.0 cm wide, and 0.6 cm thick. (The specimen thickness was dictated by the thickness of the polycarbonate sheet available for making the specimens.) With one exception, the specimens were unnotched.

The hammer of the impact machine was instrumented with a dynamic load cell which is processed to yield the stress history in the specimen as well as the total energy absorbed by the specimen.

Dynamic mechanical measurements were made using a torsional pendulum following the design of Nielsen.[1] In this measurement, a test specimen 10 × 1.6 × 0.8 cm^3 in size is manually excited into free oscillations at approximately 1 Hz. These oscillations are recorded on a strip chart recorder as damped sine waves. From the damped sine waves, two mechanical properties are obtained—shear modulus and shear loss factor. Loss factor was calculated from the relation

$$\Delta = \frac{1}{n} \ln \frac{A(r)}{A(r+n)} \tag{1}$$

where $A(r)$ is the amplitude of a reference peak and $A(r+n)$ is the peak amplitude n cycles later. Shear modulus (in dyn/cm^2) is calculated from the relation

$$G = 2.35LI/CD^3\mu P^2 \tag{2}$$

where L is the length (cm) of the specimen between clamps, C is the width (cm) of the specimen, D is the thickness (cm) of the specimen, I is the moment of inertia (g-cm^2) of the oscillating system, μ is a shape factor, and P is the period (sec) of the oscillations. Measurements were made from −196 to 150°C.

RESULTS

Fracture Topography

Fracture surfaces were gold plated and examined in a scanning electron microscope. In general, the fracture surfaces are not significantly different from those of other brittle polymers of widely different chemical structure and secondary transitions. Wolock and Newman[4] have reached a similar conclusion.

No significant differences were observed between specimens fractured at temperatures between −196 and −130°C. For temperatures above −130°C, the specimens were ductile. They bent but did not break (so there was no fracture surface to examine). Thus, the brittle-to-ductile transition temperature under impact conditions is −130°C. In a slow speed test, however, the brittle-to-ductile transition temperature has been reported[5] to be −196°C or less. (This transition is not to be confused with the secondary transition to be discussed below.)

In an unnotched test, fracture initiates at a flaw, which may be anywhere on or just beneath the surface. There is a circular slow crack growth around the flaw in what is called the mirror region, because it is rather featureless and has high specular reflectivity.[4] The mirror grows to the point where crack growth becomes unstable and starts to propagate rapidly on different levels with repeated forking, giving the surface a rough appearance.

Figure 1 illustrates a case, at −196°C, where the mirror is centered on the surface, near the middle of the specimen. In other cases, the mirror was centered

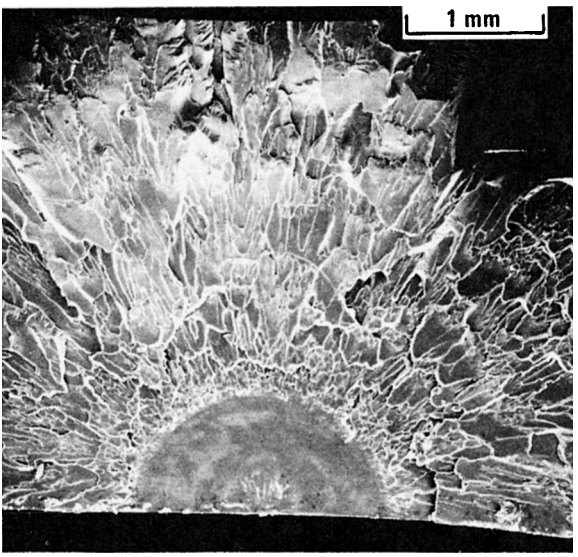

Fig. 1. Fracture initiation topography.

at a corner of the surface or as much as 1 mm below the surface. In all cases, the mirror diameter is about 2 mm.

While the region outside the mirror is very rough overall, there are some small smooth regions that contain the classic geometric fracture markings in polymers,[4] resembling a conic section (parabola, hyperbola, or ellipse), as shown in Figure 2, at −196°C. In this region the stress is sufficient to actuate secondary flaws well in advance of the main crack front. The boundary of the geometric figure represents the level difference between the main fracture plane and the secondary fracture plane. If the secondary front propagates slower than the primary front, an ellipse results, as seen in Figure 2. On this figure examination at higher magnification shows that the regions just inside or outside the ellipse are featureless down to a size of 0.1 μm.

Another regular pattern, previously reported for polystyrene in tensile fracture, is the so-called "mackerel" pattern. Figure 3, taken in the interior of a specimen fractured at −160°C, shows a similar pattern in polycarbonate with a rib spacing of about 8 μm.

While most of the measurements reported here were done on unnotched specimens, there were a few measurements made on notched specimens at room temperature. The fracture topography observed is similar to that found by Hull and Owen,[7] also on notched polycarbonate specimens.

Based on the above results, it would appear that fracture topography is not correlated with the secondary transition or temperature (in the range of −196 to −130°C), and notched fracture is significantly different than unnotched fracture.

Impact Histories

Impact measurements on polymers have been traditionally of the Izod type (cantilever beam) or Charpy type (three-point bending), in which the single figure of merit has been the total energy to fracture. Realizing the limitations of these tests, "instrumented" impact tests have become increasingly popular in the last

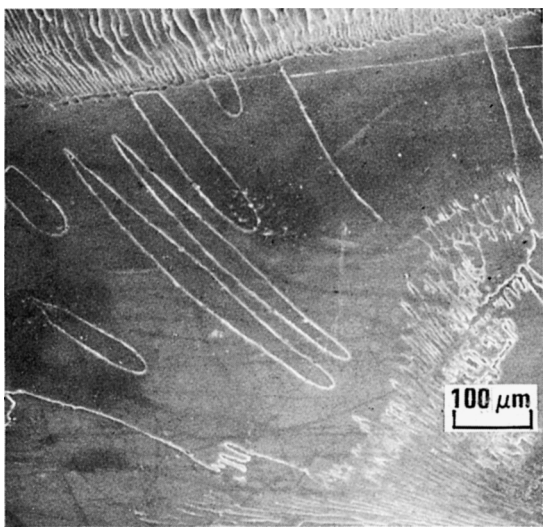

Fig. 2. Geometric fracture patterns.

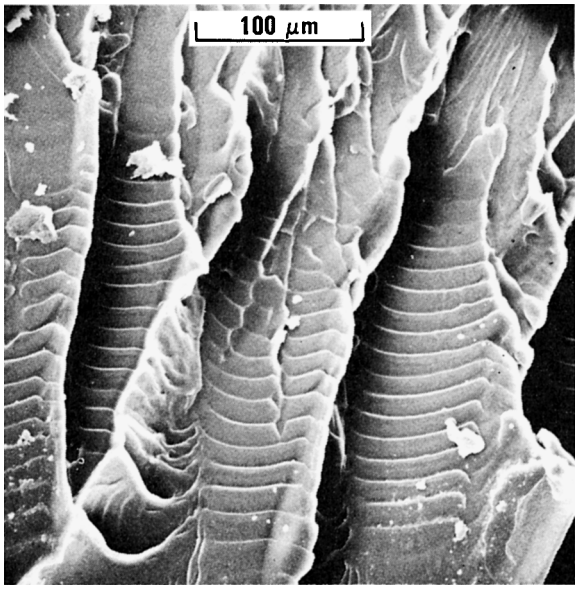

Fig. 3. Mackerel fracture patterns.

decade.[8–11] In these tests the pendulum head is equipped with a strain gauge transducer which gives an oscilloscope display of the stress history in the specimen and also the absorbed energy history.

Stress histories in polymers generally fall into one of three idealized categories[9]: brittle, ductile, and slow crack propagation, as shown schematically in Figure 4. In idealized brittle response, the stress increases nearly linearly with time, but with some softening at the higher stresses, until fracture, at which point the stress drops rapidly to zero. In ductile response, the stress reaches a maximum, showing even more softening than the brittle case, and becomes constant as the material undergoes plastic flow up to the ultimate elongation limit of the polymer where fracture occurs and the stress again drops rapidly to zero. In slow crack propagation, the initial part of the curve is similar to the ductile curve, but this is followed by a gradual tapering off of the stress as a result of stress relaxation. Fracture need not occur.

The type of stress history observed for polycarbonate changes with temperature. At − 196°C, the stress history is very nearly idealized brittle fracture, as shown in Figure 5. Some softening is observed, but fracture is catastrophic and the stress drops to zero in just 80 μsec. At −160°C, the stress history is very similar to idealized ductile response, as shown in Figure 4(b). As the temperature is raised even higher, the stress history becomes more like idealized slow crack growth, as shown in Figure 6, at room temperature. (Recall that at this temperature the specimen did not break but bent into a "vee" shape.)

The stress histories obtained here are qualitatively similar to those obtained on polycarbonate in Izod impact studies[8,11] as well as Izod impact studies on other polymers[8,9] and even on aluminum.[10]

Energy histories were also obtained on all specimens. The total energy required to produce failure as a function of test temperature is shown in Figure 7. Note that there is a definite peak in energy at about −70°C.

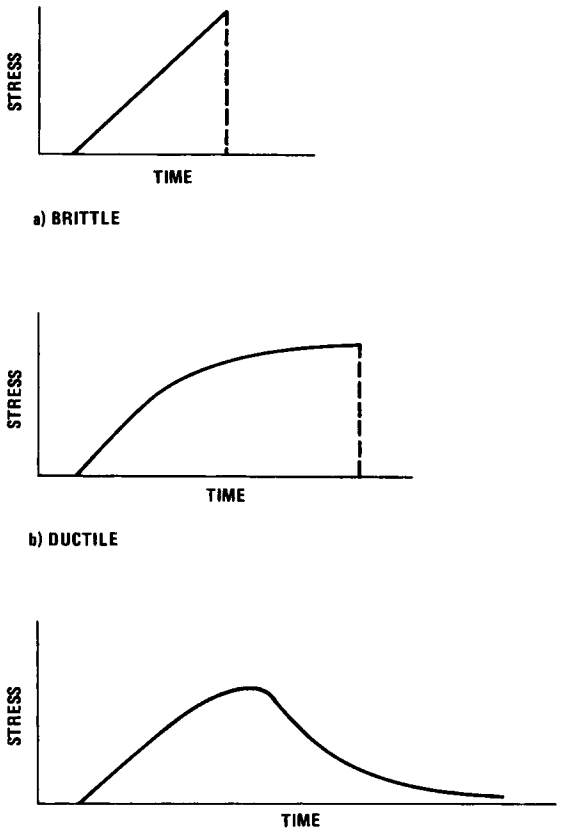

Fig. 4. Idealized impact stress histories.

Fourier Transforms

It has already been pointed out that it is important to compare impact and viscoelastic losses at the same temperature and frequency.[2,3] Even though the secondary transition in polycarbonate occurs well below room temperature at 1 Hz, high-speed impact at room temperature is equivalent to a higher frequency measurement, which shifts the secondary loss peak to higher temperature. Sacher[2] used the rise time of a stress history similar to Figure 5 to calculate an equivalent frequency for impact. He calculated a single frequency of 5 kHz to represent the impact. In this paper we calculate the complete frequency distribution produced by impact by looking at the Fourier spectrum of the stress history.

In general, the Fourier spectrum of a stress history, $\sigma(t)$, is given by

$$S(\omega) = \int_{-\infty}^{\infty} \sigma(t)\, e^{-i\omega t}\, dt \tag{3}$$

where ω is the circular frequency ($\omega = 2\pi f$). For the cases of interest here, the stress history has a definite beginning and end, taken as 0 and D. Therefore eq. (3) becomes

$$S(\omega) = \int_{0}^{D} \sigma(t)\, e^{-i\omega t}\, dt \tag{4}$$

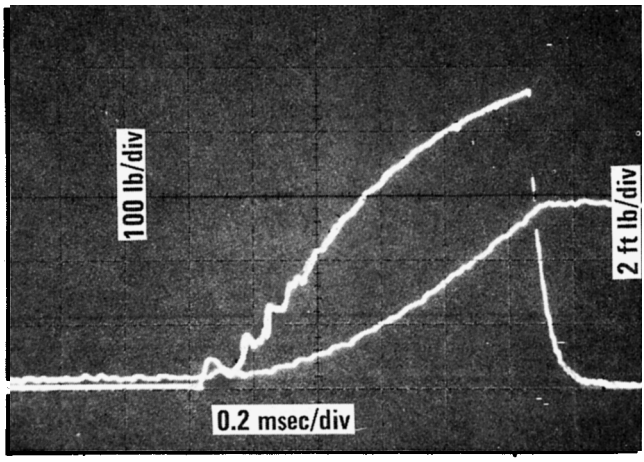

Fig. 5. Impact stress history at −196°C.

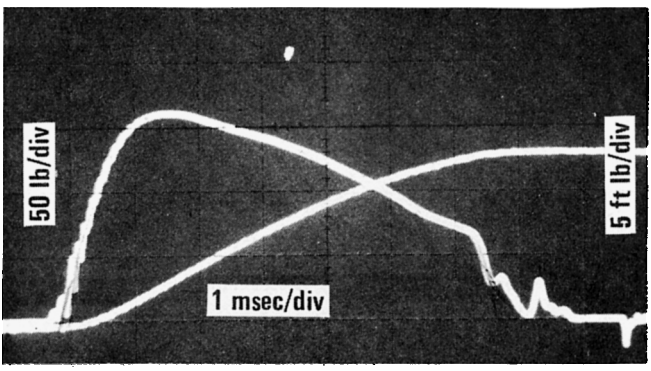

Fig. 6. Impact stress history at room temperature.

This integral can be evaluated analytically for the case of idealized brittle behavior, Figure 4(a). The normalized magnitude of the Fourier spectrum is defined as

$$S_N = |S|/|S|_0 \tag{5}$$

where $|S|_0$ is the magnitude of the spectrum at zero frequency. For idealized brittle behavior, then,

$$S_N = \frac{2}{\omega D}\left[1 - \frac{2\sin(\omega D)}{\omega D} + \frac{4\sin^2(\omega D/2)}{(\omega D)^2}\right]^{1/2} \tag{6}$$

This spectrum can be plotted in terms of reduced frequency, ωD, as shown in Figure 8. The spectrum has a maximum at zero frequency and decreases to a shallow local minimum at $\omega D = 8$. At higher frequency, the spectrum gradually decreases with superimposed periodic oscillations. In short, the Fourier spectrum of an impact pulse is composed of a broad distribution of frequencies that extends from zero to high frequency.

The measured impact pulse at −196°C (Fig. 5) was used in eq. (4) and integrated numerically with the result which is also shown in Figure 8. The spectrum is slightly broader than the idealized case (i.e., has more high-frequency com-

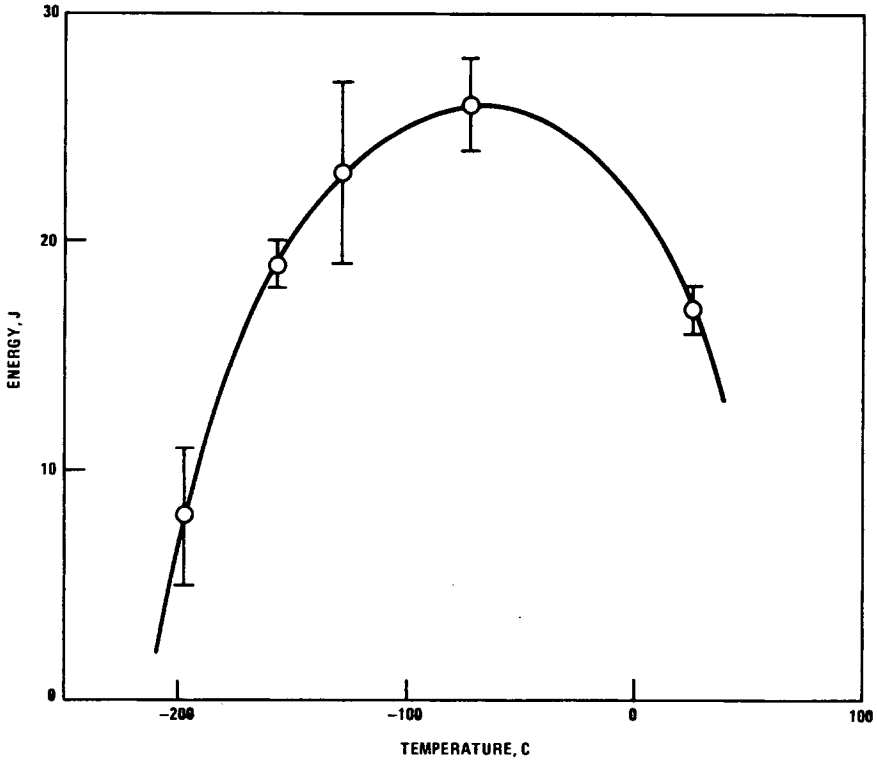

Fig. 7. Failure energy vs test temperature.

ponents) but is not significantly different than the idealized brittle response. From Figure 5 the impact duration D is 1.08 msec, so the first minimum (ωD = 8) occurs at 1200 Hz. The frequency used by Sacher,[2] 5 kHz, occurs at a reduced frequency of ωD = 34, i.e., much higher than the range of the most important frequencies (those with the biggest magnitude).

The measured stress history at room temperature (Fig. 6) was also integrated numerically, with the result shown in Figure 8. While the pulse duration is much longer (D = 6.6 msec) than the duration at −196°C and the pulse shape is quite different, the normalized spectrum as a function of reduced frequency is very similar. In this case the first minimum occurs at 200 Hz.

As expected, the Fourier spectrum of an impact pulse does not consist of a single frequency but of a broad distribution of frequencies. While this distribution of frequencies extends to very high frequency, the most important contributions at room temperature are below 200 Hz.

Dynamic Mechanical Loss Factor

Dynamic mechanical loss factor measurements were made using a torsional pendulum, with results shown in Figure 9. There is a glass transition at about 150°C and a secondary transition at −105°C. The locations of these peaks are in good agreement with the measurements of others.[12-14] While the broad secondary transition peak has been resolved[15] into multiple peaks, which are

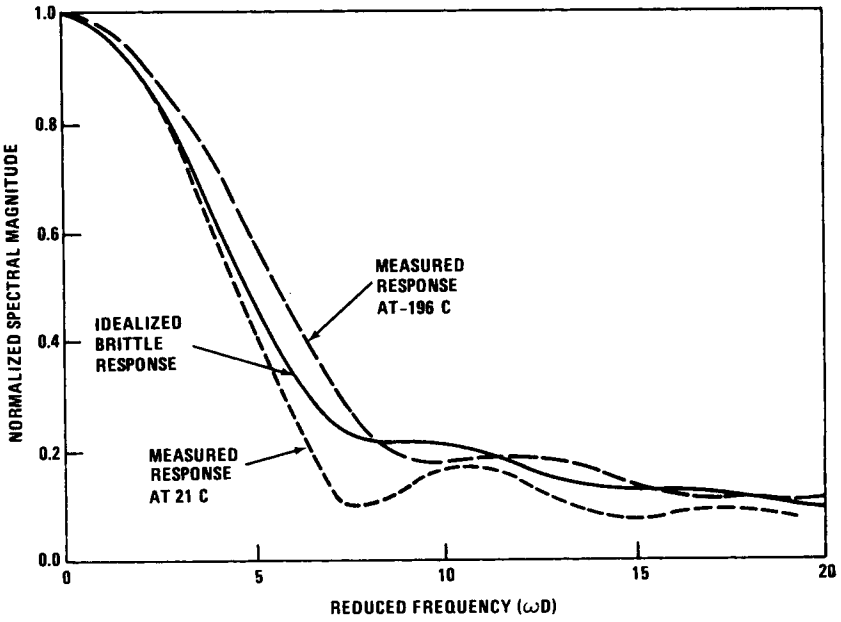

Fig. 8. Normalized spectral magnitude vs reduced frequency.

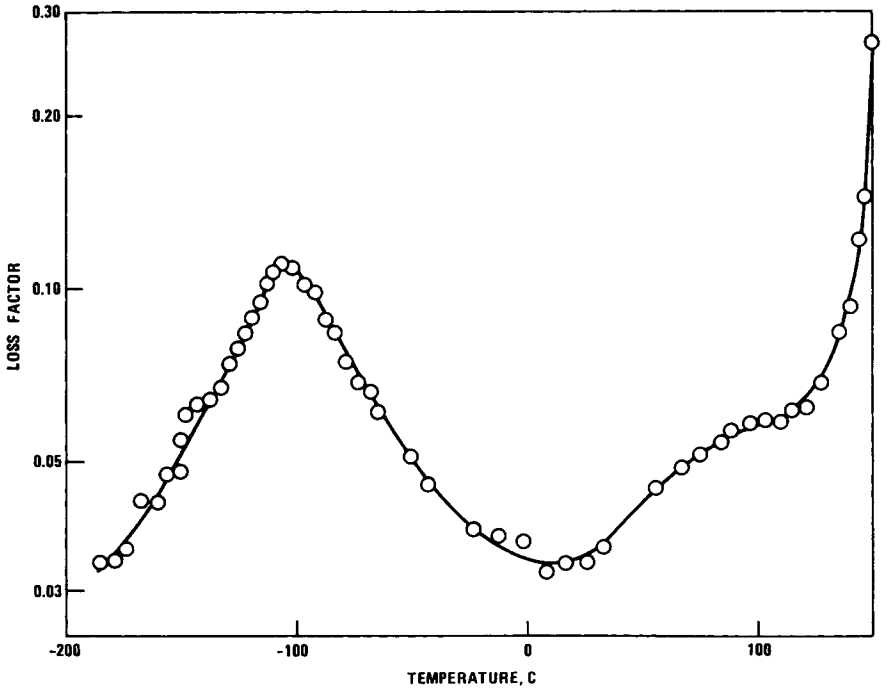

Fig. 9. Loss factor vs temperature at 1.3 Hz.

suggested by shoulders on the peak in Figure 9, we will ignore this fine structure and consider the peak as one transition.

The torsional pendulum measurements are made as a function of temperature

at one frequency, 1.3 Hz. We wish now to determine what the frequency distribution of the secondary transition is at room temperature using the time–temperature superposition principle. In the glassy state, where secondary transitions occur, the relation between measurements made as a function of absolute temperature T at a fixed frequency f_0 and measurements made at a fixed temperature T_0 as a function of frequency f is given by an Arrhenius equation[16]

$$\ln (f/f_0) = (\Delta H/R)[(1/T) - (1/T_0)] \tag{7}$$

where ΔH is the activation energy and R is the gas constant.

To convert torsional pendulum temperature measurements at $f_0 = 1.3$ Hz to frequency data at any given T_0 using eq. (7), the activation energy must be known. This quantity can be estimated from the data on Figure 9 by integrating the area under the secondary transition peak,[17] with the result that $\Delta H = 15 \pm 3$ kcal/mole. Phillips, North, and Pethrick[18] have made a comprehensive survey of literature values of mechanical and dielectric measurements on the secondary transition in polycarbonate covering eight decades of frequency. They find an average value from all workers of $\Delta H = 10 \pm 1$ kcal/mole. This agreement is considered satisfactory, and $\Delta H = 15$ kcal/mole will be used in this paper. (Using the lower value does not change any of the conclusions reached here.)

Using eq. (7) and Figure 9 shows that the secondary transition frequencies at room temperature cover a very broad range of frequencies centered at about 7 MHz. This peak frequency is close to that calculated by Boyer.[3] As the test temperature decreases, the damping peak shifts to lower frequency.

Picking 100 Hz as the average frequency generated on impact, the loss factor versus temperature can be calculated at that frequency, with the result shown in Figure 10. The secondary peak has shifted to −80°C from its original value of −105°C (at 1.3 Hz). Note that the absorption peak occurs at very nearly the same temperature that the impact energy has a peak (Fig. 7). This close correlation is direct evidence that the secondary transition governs the impact resistance of polycarbonate rather than, for example, free volume theories that do not predict a peak in impact strength. Vincent[19] has obtained similar results for notched specimens of various polymers.

The above correlation was made at a single frequency. A more detailed analysis can be done by comparing the frequency spectrum of the impact pulse and the frequency spectrum of the secondary transition. This comparison is expected to be qualitative rather than quantitative. One reason is that the damping factor that is measured in the torsional pendulum is the shear damping factor while the appropriate damping for impact would either be longitudinal or some combination of shear and longitudinal. Also, the shear damping factor was determined at relatively small strain while impact goes into the finite strain region. While it has been suggested[20] that the damping factor in polycarbonate is independent of strain even into the large strain region, this has not been demonstrated. There should at least be a qualitative relation though between the damping factor measured in the torsional pendulum and the damping of impact-generated stress waves in the polycarbonate.

The significant frequencies generated by impact are those up to $\omega D = 8$, which for room-temperature impact corresponds to a frequency of 200 Hz. As shown in Figure 11, the secondary transition absorption is moderately high in this region.

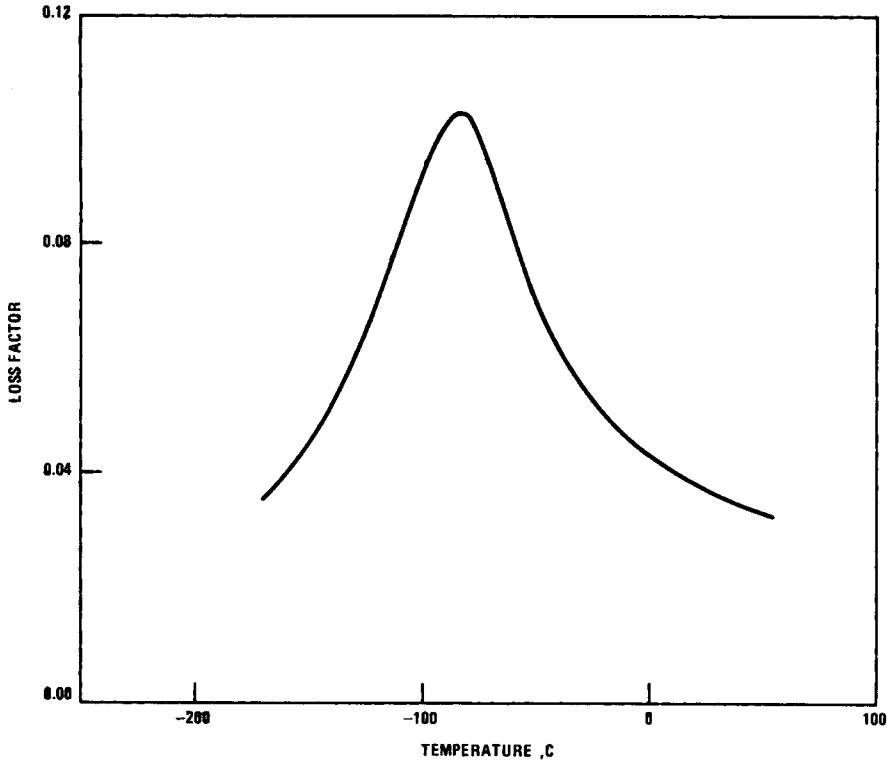

Fig. 10. Loss factor vs temperature at 100 Hz.

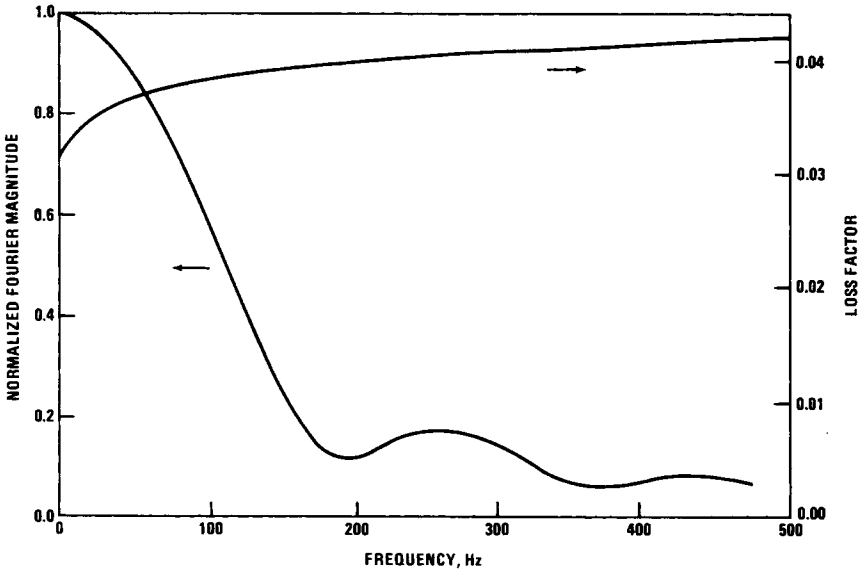

Fig. 11. Fourier magnitude and loss factor vs frequency. T = 21°C; pulse duration, 6.6 msec.

Note that the absorption is decreasing at low frequency, and at extremely low frequency the absorption increases markedly owing to the glass transition, but all this will have little effect on damping the impact pulse. Figure 11, then, is a qualitative demonstration of why a secondary transition is related to impact

at room temperature. As previously noted, the absorption, and consequently impact strength, will be even higher at lower temperature.

CONCLUSIONS

Instrumented Charpy impact measurements were made on a polycarbonate as a function of temperature. Fracture surfaces were examined in a scanning electron microscope. Measurements were also made in a torsional pendulum as a function of temperature. Based on an analysis of these measurements, we have reached the following conclusions:

1. Fracture topography is not directly correlated with either the secondary transition or temperature.
2. Notched fracture is significantly different than unnotched fracture.
3. The transition from brittle fracture to ductile failure occurs at −130°C.
4. Impact strength has a maximum at −70°C.
5. The Fourier spectrum of room temperature impact extends to 200 Hz.
6. At room temperature, the secondary transition occurs over a broad frequency range peaked at 7 MHz.
7. The secondary transition peak rises 25°C due to the higher frequency of impact.
8. The secondary transition peak at 100 Hz has a maximum at −80°C.
9. Secondary transitions are directly correlated with the impact resistance of polymers.

The authors wish to thank R. G. Hayes (Naval Surface Weapons Center) and Dr. D. R. Ireland (Effects Technology, Inc.) for their help in making impact measurements, and Dr. M. K. Norr (Naval Surface Weapons Center) for making the scanning electron micrographs.

References

1. L. E. Nielsen, *Mechanical Properties of Polymers and Composites,* Marcel Dekker, New York, 1974, p. 218.
2. E. Sacher, *J. Macromol. Sci.-Phys. B, 11,* 403 (1975).
3. R. F. Boyer, *Polymer,* **17,** 996 (1976).
4. I. Wolock and S. B. Newman, in *Fracture Processes in Polymeric Solids,* B. Rosen, Ed., Interscience, New York, 1964, pp. 235–290.
5. E. H. Andrews, *Fracture in Polymers,* American Elsevier, New York, 1968, p. 53.
6. J. Murray and D. Hull, *J. Polym. Sci. A-2,* **8,** 583 (1970).
7. D. Hull and T. W. Owen, *J. Polym. Sci.–Phys.,* **11,** 2039 (1973).
8. W. E. Wolstenholme, *J. Appl. Polym. Sci.,* **6,** 332 (1962).
9. C. B. Arends, *J. Appl. Polym. Sci.,* **9,** 3531 (1965).
10. D. R. Ireland, *ASTM Special Technical Publication 563,* 1974, pp. 3–29.
11. H. Gonzalez, *J. Appl. Polym. Sci.,* **19,** 2717 (1975).
12. F. P. Reding, J. A. Faucher, and R. D. Whitman, *J. Polym. Sci.,* **54,** 556 (1961).
13. I. I. Perepechko, L. A. Kvacheva, and I. I. Levantovskaya, *Polym. Sci. (USSR) A,* **13,** 702 (1971).
14. I. I. Perepechko and O. V. Startsov, *Sov. Phys. Acoust.,* **20,** 456 (1975).
15. Y. Aoki and J. O. Brittain, *J. Polym. Sci., Phys.,* **15,** 199 (1977).
16. J. D. Ferry, *Viscoelastic Properties of Polymers,* 2nd ed., Wiley, New York, 1970.
17. N. G. McCrum, B. E. Read, and G. Williams, *Anelastic and Dielectric Effects in Polymeric Solids,* Wiley, New York, 1967, p. 124.
18. D. W. Phillips, A. M. North, and R. A. Pethrick, *J. Appl. Polym. Sci.,* **21,** 1859 (1977).
19. P. I. Vincent, *Polymer,* **15,** 111 (1974).
20. W. W. Gerberich and G. C. Martin, *J. Polym. Sci.–Phys.,* **14,** 897 (1976).

Received May 9, 1978
Revised October 16, 1978